Cooperative interaction of Angiopoietin-like proteins 1 and 2 in zebrafish vascular development

Yoshiaki Kubota*, Yuichi Oike*†, Shinya Satoh‡, Yoko Tabata‡, Yuichi Niikura‡, Tohru Morisada*, Masaki Akao*, Takashi Urano*, Yasuhiro Ito*, Takeshi Miyamoto*, Norihiro Nagai*, Gou Young Koh§, Sumiko Watanabe‡, and Toshio Suda*†

*Department of Cell Differentiation, The Sakaguchi Laboratory, School of Medicine, Keio University, 35 Shinanomachi, Shinjuku-ku, Tokyo 160-8582, Japan; ‡Division of Molecular and Developmental Biology, Institute of Medical Science, University of Tokyo, Minato-ku, Tokyo 108-8639, Japan; and §Biomedical Research Center and Department of Biological Sciences, Korea Advanced Institute of Science and Technology, 373-1 Guseong-dong, Yuseong-gu, Daejeon 305-701, Republic of Korea

Edited by George D. Yancopoulos, Regeneron Pharmaceuticals, Inc., Tarrytown, NY, and approved July 5, 2005 (received for review March 8, 2005)

Angiopoietin-like protein (Angptl) 1 and Angptl2, which are considered orphan ligands, are highly homologous, particularly in the fibrinogen-like domain containing the putative receptor binding site. This similarity suggests potentially cooperative functions between the two proteins. In this report, the function of Angptl1 and Angptl2 is analyzed by using morpholino antisense technology in zebrafish. Knockdown of both Angptl1 and Angptl2 produced severe vascular defects due to increased apoptosis of endothelial cells at the sprouting stage. *In vitro* studies showed that Angptl1 and Angptl2 have antiapoptotic activities through the phosphatidylinositol 3-kinase/Akt pathway, and coinjection of constitutively active Akt/protein kinase B mRNA rescued impaired vascular development seen in double knockdown embryos. These results provide a physiological demonstration of the cooperative interaction of Angptl1 and Angptl2 in endothelial cells through phosphatidylinositol 3-kinase/Akt mediated antiapoptotic activities.

angiogenesis | morpholino | phosphatidylinositol 3-kinase | Akt | apoptosis

Development of the vascular system occurs as two distinct processes, vasculogenesis and angiogenesis. In vasculogenesis, hemangioblasts derived from the lateral plate mesoderm form tubular structures of the primary vasculature. In angiogenesis, new vessels sprout from preexisting vasculature and are further remodeled to form mature blood vessels. Angiogenesis consists of several activities of endothelial cells, such as migration and apoptosis. Angiopoietin signaling through the Tie2 receptor is widely known to play a key role in angiogenesis (1–7).

Angiopoietin (Ang) 1 and all members of the angiopoietin family possess two characteristic structures: a coiled-coil domain, which likely contributes to oligomerization, and a fibrinogen-like domain, thought to contain the receptor binding site. Recently, we (8–10) and others (11–15) identified several genes encoding proteins containing both the coiled-coil domain and the fibrinogen-like domain. Although these factors were initially predicted to function as ligands for Tie receptors, they bound neither Tie1 nor Tie2. Therefore, they are currently orphan ligands and designated angiopoietin-like proteins (Angptls) or angiopoietin-related proteins (ARPs). Several studies show that Angptl/ARP family proteins possess potent activities in the vascular system (8–16). Angptl1 and Angptl2 have been reported to possess weak endothelial cell-sprouting activities (11, 12); however, there is little information as to their physiological functions.

Zebrafish offer several advantages as a model system for analyzing vascular development. One reason is that rapid external development of a transparent embryo permits visual analysis of phenotypic defects. Not only vascular structures but also apoptotic cells can be clearly visualized in whole-mount specimens (17, 18). Indeed, zebrafish has been used to investigate several vascular processes, particularly commitment of hemangioblasts (19, 20) and arterial-venous identification (21–24). Recently, we cloned the zebrafish orthologues of Angptl1 and Angptl2 (*Zangptl1* and *Zangptl2*, respectively) (25). Based on the results of a syntenic search by using the genome database and comparing expression patterns between zebrafish and mammals in adult tissues, we determined our isolated *Zangptl1* and *Zangptl2* are the orthologues of their mammalian counterparts, respectively. In that report, we also described their embryonic expression patterns. Both *Zangptl1* and *Zangptl2* are expressed mainly in the caudal part of the corpus at ≈24 h after fertilization (hpf) when angiogenesis manifested by sprouting of intersomitic vessels (ISVs) occurs. *Zangptl1* is expressed in the myotome, and *Zangptl2* is predominantly expressed in the yolk sac extension, especially in the yolk syncytial layer and the spinal cord, suggesting that both factors might act on endothelial cells of ISVs sprouting toward such structures. To examine the physiological functions of both genes simultaneously, we used a loss-of-function strategy by using morpholinos, an antisense technology widely used to knockdown multiple genes predicted to act cooperatively (26, 27). Our studies indicate that both Angptl1 and Angptl2 possess antiapoptotic activity through the phosphatidylinositol 3-kinase (PI3-K)/Akt pathway and that their cooperative activities are required for vascular development in zebrafish embryogenesis.

Materials and Methods

Zebrafish Maintenance. Zebrafish were kept at standard conditions (28). Embryos >24 hpf were raised in 0.2 mM 1-phenyl-2-thio-urea (Sigma) to prevent pigment formation.

Morpholino Sequences. Morpholinos (Gene Tools, Philomath, OR) were targeted to 25 bases around the start codons or 5′-UTR of *Zangptl1* and *Zangptl2*. They have the following sequences: the first *Zangptl1* morpholino, (Angptl1mo), 5′-CCATGCACCACGTTACACCTCT*CAT*-3′ (antisense for the start codon is underlined); 5-base mismatch morpholino of Angptl1mo (Angptl1d5), 5′-CCATcCAgCACcTTACACgTCTgAT-3′ (mismatched bases are indicated by small letters); the second *Zangptl1* morpholino, (Angptl1mo2) designed in the 5′-UTR of *Zangptl1*, 5′-TACTTCTGTTATCACCTCACAGGGT-3′; the first *Zangptl2* morpholino, (Angptl2mo), 5′-CTAGTGAAGGAACATC*CAT*GACCAC-3′ (antisense for the start codon is underlined); 5-base mismatch morpholino of

This paper was submitted directly (Track II) to the PNAS office.

Abbreviations: Ang, angiopoietin; Angptl, angiopoietin-like protein; DA, dorsal aorta; DMO, double morpholino; ERK, extracellular signal-regulated kinase; hpf, h after fertilization; HUVEC, human umbilical vein endothelial cell; ISH, *in situ* hybridization; ISV, intersomitic vessels; PKB, protein kinase B; St, standard morpholino-injected group; Zangptl*n* morphino, zebrafish orthologues of Angptl *n*.

†To whom correspondence may be addressed. E-mail: oike@sc.itc.keio.ac.jp or sudato@sc.itc.keio.ac.jp.

Angptl2mo (Angptl2d5), 5′-CTAGTcAAcGAAgATCCATcACgAC-3′ (mismatched bases are indicated by small letters); and the second *Zangptl2* morpholino, (Angptl2mo2) designed in 5′-UTR of *Zangptl2*, 5′-CACCAGATGATCCCAGGCTATTGCA-3′.

Microinjections. Morpholinos and/or mRNA were diluted to the indicated concentrations with Danieau buffer (58 mM NaCl/0.7 mM KCl/0.4 mM $MgSO_4$/0.6 mM $Ca(NO_3)_2$/5.0 mM Hepes, pH 7.6) and ≈2 nl were injected into the yolk of one- to four-cell stage embryos. The standard control morpholino available from Gene Tools was used as an injection control.

Microangiography. Microangiography was performed as described in ref. 29. Briefly, FITC-Dextran in Danieau buffer at 2 mg/ml was injected into the sinus venosa/cardinal vein of anesthetized embryos. Photographs were taken during observation under a Leica MZFL III dissection microscope equipped with the standard FITC filter set.

Whole-Mount *in Situ* Hybridization (ISH). Probes for flk-1, fli-1, myoD, and nkx2.5 genes were cloned by PCR amplification. PCR products were subcloned into the pGEM T-easy vector. Digoxigenin (DIG)-labeled antisense RNA probes were synthesized by using a DIG RNA labeling kit (Roche Diagnostics, Mannheim, Germany). Whole-mount ISH was performed as described in ref. 30.

Whole-Mount TUNEL Staining. Embryos were fixed in 4% paraformaldehyde at 4°C overnight before staining by using the ApopTag Peroxidase *In Situ* Apoptosis Detection kit (Chemicon, Temecula, CA) according to the manufacturer's instructions, essentially as described in refs. 17 and 31.

Synthesis of Recombinant COMP-Angptl1 and -Angptl2 Proteins. To investigate the role of Angptl1 and Angptl2 directly, we generated their recombinant proteins. Notably, we designed the Angptl1 variant, COMP-Angptl1, in which the fibrinogen-like domain of mouse Angptl1 was fused to the coiled-coil domain of rat cartilage oligomeric matrix protein (DLAPQMLRELQETNAALQDVRELLRQQVKEITFLKNTVMECDACG) to avoid aggregation and insolubility of Angptl1. COMP-Angptl1 and the native form of mouse Angptl2 fused at the amino terminus to the FLAG epitope were subcloned into pCEP4 (Invitrogen, Groningen, The Netherlands), and recombinant FLAG-tagged proteins (COMP-Angptl1-FLAG and Angptl2-FLAG) were purified as described in refs. 8 and 10. The proteins obtained were visualized by Western blotting with horseradish peroxidase-conjugated anti-FLAG antibody (M2) (Sigma) (see *Supporting Materials and Methods*, which is published as supporting information on the PNAS web site).

Cell Culture. Human umbilical vein endothelial cells (HUVECs) were cultured in EGM-2 medium obtained from Cambrex (East Rutherford, NJ) as described in ref. 32. The murine pro-B cell line BaF/3 was maintained in RPMI medium 1640 (GIBCO/BRL, Grand Island, NY) supplemented with 10% FCS (GIBCO) and 1 ng/ml IL-3 (Wako, Osaka). The hepatoma line Fao was maintained in low glucose-DMEM (GIBCO/BRL) supplemented with 10% FCS.

Binding Assay. Cells were resuspended and incubated in PBS with 5% FCS including either FLAG-tagged or biotinylated COMP-Angptl1 and Angptl2 for 30 min on ice. In some experiments, cells were preincubated in PBS with 5% FCS including indicated proteins at the same concentration for 15 min on ice before the primary incubation. Immunodetection of cells bound by COMP-Angtl1 or -Angptl2 was accomplished with FITC-conjugated anti-FLAG antibody or Streptavidin. Stained cells were analyzed by using a FACScan cytometer and CELLQUEST software (Becton Dickinson, Franklin Lakes, NJ), and the mean fluorescent intensity was monitored and calculated as the ratio in comparison with the vehicle-treated cells.

Phosphorylation Assay of Extracellular Signal-Regulated Kinase (ERK)1/2 and Akt. Cells were starved in their respective maintenance medium without serum and growth factors for 12 h (HUVECs and Fao) or 4 h (BaF/3) and stimulated with 0.5 μg/ml COMP-Angptl1 or -Angptl2 proteins for various times. Phosphorylation assays of ERK1/2 and Akt were performed as described in ref. 32.

TUNEL Assay of HUVECs. For TUNEL assays, HUVECs were cultured in serum-free medium in the presence of either vehicle (PBS) or 0.5 μg/ml COMP-Angptl1 or -Angptl2. In some experiments, cells were incubated with the MEK inhibitor, PD980059 (Biomol, Plymouth Meeting, PA) (5 μg/ml) or the PI3-K inhibitor, LY294002 (Calbiochem, San Diego) (5 μg/ml). As controls in the inhibitor experiments, equivalent amounts of DMSO vehicle were added to the medium. Apoptotic adherent cells were stained by using an ApopTag Fluorescein *In Situ* Apoptosis Detection Kit (Chemicon). Nuclear staining was done by TOTO3. Cells were observed under a fluorescent microscope.

Synthesis of Myristoylated Akt/Protein Kinase B (PKB) mRNA. To prepare the active form of Akt-1/PKBα mRNA, myristoylated human AKT-1/PKBα cDNA (kindly provided by Dr. Kenneth Walsh, Boston University, Boston), which has been reported to have high homology with a zebrafish orthologue and function in zebrafish *in vivo* (17), was linearized at the 3′ end, and capped RNAs were *in vitro* transcribed by using the Message Machine Kit (Ambion, Austin, TX) as described in refs. 17 and 33.

Results

Loss of Angptl1 and Angptl2 Promotes Vascular Defects. To evaluate the physiological effect of Angptl1 and Angptl2, we undertook loss-of-function experiments in zebrafish by using morpholinos. Our first observation was embryonic lethality at 72 hpf caused by pericardial effusion. Although the number of embryos with pericardial effusion showed a dose-dependent increase in the Angptl1mo- (Angptl1MO) and Angptl2mo- (Angptl2MO) injected group compared with the standard morpholino-injected group (St), the group injected with both Angptl1mo and Angptl2mo (double morpholino, DMO) showed remarkable increases in the number of embryos with pericardial effusion (Fig. 1*A*; see also Fig. 5, which is published as supporting information on the PNAS web site). To determine whether defects in heart development occurred at earlier stages, we examined expression of *nkx2.5* and found normal expression in DMO embryos (Fig. 6, which is published as supporting information on the PNAS web site). At 48 hpf, when the heartbeat can be easily observed, the DMO group showed a normal heartbeat similar to the St group (Movies 1 and 2, which are published as supporting information on the PNAS web site). To determine whether pericardial effusion was attributable to defects in vascular development, we observed blood flow in the same embryos. Interestingly, although we detected blood flow in two major trunk vessels, the dorsal aorta (DA) and postcardinal vein, in both St and DMO groups, we could not detect blood flow in ISVs and the dorsal-longitudinal anastomosus vessel in the DMO group as detected in the St group (Movies 3 and 4, which are published as supporting information on the PNAS web site), suggesting that vascular defects precede heart defects. To visualize blood vessel formation at this stage, we performed angiography (Fig. 1*B*) and ISH for fli-1 (Fig. 1*C*). Although the major trunk vessels were clearly detected, ISVs and dorsal-longitudinal

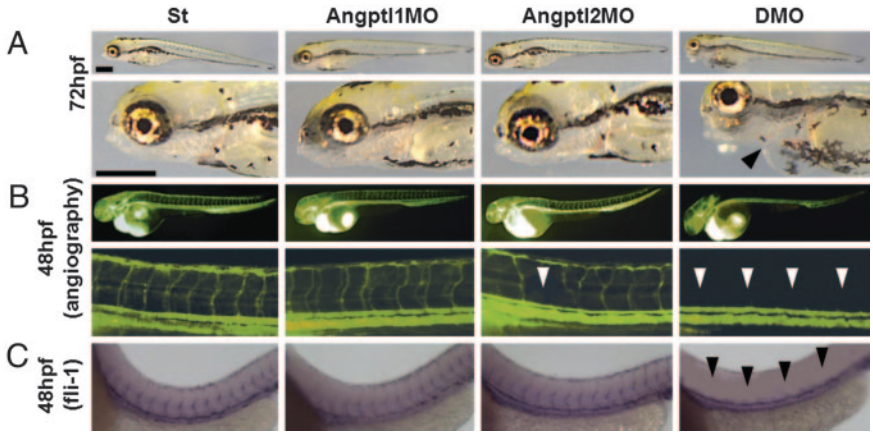

Fig. 1. Vascular defects observed in Angptl1 and Angptl2 double knockdown embryos. (*A*) Representative photographs of simple microscopic observation of 72 hpf embryos St, Angptl1MO, Angptl2MO, and DMO groups. The lower four photographs are high magnifications of the upper four. A closed arrowhead indicates pericardial effusion seen especially in DMO groups (Scale bar: 400 μm.). (*B*) Representative photographs of angiography at 48 hpf. The lower four photographs are high magnifications of the upper four. Open arrowheads indicate the absence of blood flow in ISVs and dorsal-longitudinal anastomosus vessels. (*C*) Representative photographs of whole-mount ISH of fli-1 at 48 hpf. Filled arrowheads indicate absence of ISVs and dorsal-longitudinal anastomosus vessels in DMO.

anastomosus vessels was undetectable in the DMO group in both experiments. These findings suggest that impaired vascular development is the primary defect seen when Angptl1 and Angptl2 activity is lost.

Loss of Angptl1 and Angptl2 Promotes Impaired Sprouting of ISVs and Increased Numbers of Apoptotic Cells Around DA. To determine the initiation of vascular defects in DMO, we examined vascular development at early developmental stages by whole-mount ISH of endothelial markers. Vascular defects were first observed as impaired sprouting of ISVs as detected by ISH of flk-1 at 28 hpf. The DMO group showed complete loss of sprouting of ISVs (Fig. 2*A*). Defects of impaired sprouting vessels were quantitatively analyzed as described in refs. 18 and 27. A high percentage of the DMO group showed impaired sprouting (Fig. 7, which is published as supporting information on the PNAS web site). To confirm the specificity of these findings, we analyzed defects of sprouting vessels by using second morpholinos or morpholinos with five mismatched bases as negative controls (Fig. 8 and 9, which are published as supporting information on the PNAS web site). In both experiments, we obtained results similar to those seen with the first set of morpholinos.

The formation of hemangioblasts is a very early step in the development of the vascular system. Hemangioblasts form in the lateral plate mesoderm at 12 hpf, and tubular structures of the primary vasculature formed by the hemangioblasts at 18 hpf can be visualized by ISH of fli-1 and flk-1. Formation of such structures was normal in DMO embryos, suggesting normal

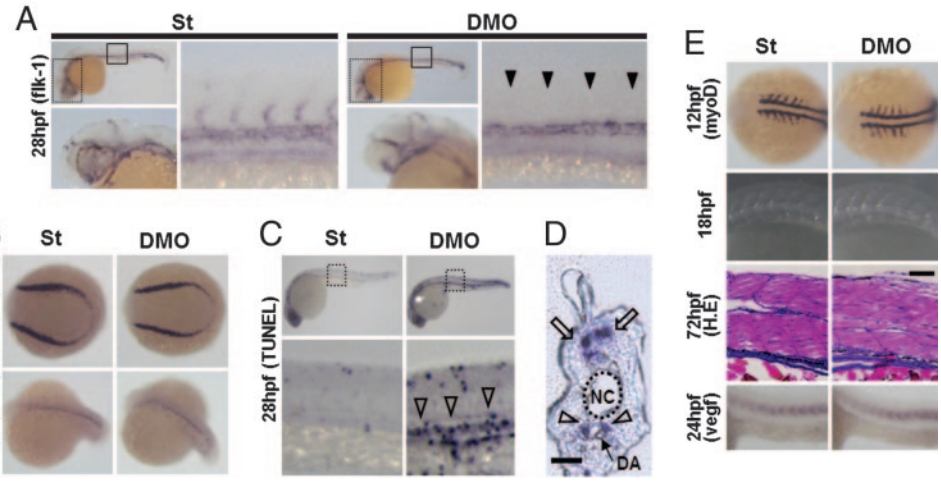

Fig. 2. Impaired sprouting of ISVs and elevated apoptotic cells around the DA are seen in DMO embryos. (*A*) Representative photographs of whole-mount ISH of flk-1 at 28 hpf in St and DMO embryos. High magnification images of head portions indicated by dotted grids in the upper left are shown in the lower left. Normal vasculature in head portion is seen in both St and DMO. High magnification images in the trunks indicated by closed grids in the upper left are shown in the right images. Filled arrowheads indicate ISVs with impaired sprouting in DMO. (*B*) Representative photographs of whole-mount ISH of fli-1 at 12 hpf and flk-1 at 18 hpf in St and DMO embryos. Normal vasculogenesis occurs in DMO-injected embryos. (*C*) Representative photographs of whole-mount TUNEL assay at 28 hpf. High magnification images of the trunk indicated by dotted grids in *Upper* are shown in *Lower*. Open arrowheads indicate increased apoptotic cells in the area of major trunk vessels in DMO. (*D*) A sagittal section of DMO embryos stained with TUNEL. Open arrowheads indicate apoptotic cells around the DA, and open arrows indicate naturally occurring apoptosis in the neural tube. NC, notochord. (Scale bar: 50 μm.). (*E*) Representative photographs of somites examined by whole-mount ISH of myoD at 12 hpf, simple microscopic observation at 18 hpf, hematoxylin/eosin staining of sagittal sections at 72 hpf, and whole-mount ISH of vegf at 24 hpf. Somitogenesis and vegf expression are not impaired in DMO embryos. (Scale bar: 100 μm.).

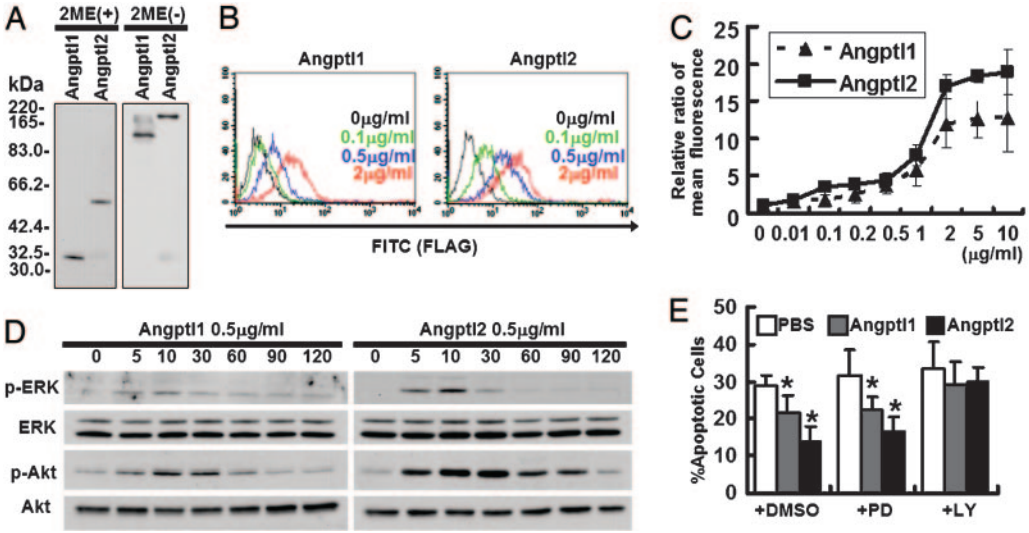

Fig. 3. Angptl1 and Angptl2 bind to endothelial cells, and possess antiapoptotic activity through the PI3-K/Akt pathway. (*A*) Western blotting analysis with an anti-FLAG antibody with (*Left*) or without (*Right*) 2-mercaptoethanol (2ME). (*B* and *C*) Binding of COMP-Angptl1-FLAG and Angptl2-FLAG to HUVECs. The FITC intensity indicates cells bound by FLAG-tagged proteins. With both COMP-Angptl1 (*Left*) and Angptl2 (*Right*), intensities increased in a dose-dependent manner with saturation at ≈2 μg/ml. (*D*) Phosphorylation assay of ERK1/2 and Akt. HUVECs were treated with COMP-Angptl1 or -Angptl2 proteins. Immunoblotting was performed with anti–pERK1/2 or anti-pAkt antibody. Total amounts of ERK1/2 or Akt proteins were monitored by reprobing membranes with anti-ERK1/2 antibody and anti-Akt antibody. (*E*) TUNEL assay. HUVECs were cultured in the presence of either vehicle (PBS) or 0.5 μg/ml of COMP-Angptl1 or -Angptl2. In some experiments, cells were incubated with DMSO or 5 μg/ml PD980059 or LY294002. Data shown is the average of 6 fields each in six independent experiments ($n = 36$). *, $P < 0.03$ (compared with PBS in each group).

vasculogenesis can occur in the absence of Angptl1 and Angptl2 (Fig. 2*B*).

To investigate the mechanism underlying impaired sprouting, we examined apoptotic cells *in vivo* by whole-mount TUNEL assay. Apoptotic cells around the DA were markedly increased in the DMO group compared with the control group (Fig. 2 C and *D*). On the other hand, there was no significant difference in the number of physiological apoptotic cells in neural tube (31) between St and DMO groups when we counted TUNEL-positive cells in the neural tube within rostral and caudal ends of yolk sac extension (17.9 ± 5.34 and 19.8 ± 5.3, respectively: $n = 7$, $P = 0.53$).

Because somitic cells secrete angiogenic factors such as VEGF, normal development of somites is essential for angiogenesis in zebrafish. Thus, we examined somitogenesis and VEGF expression in the DMO group. Somitogenesis appeared normal and no alteration in VEGF expression was observed in the DMO group (Fig. 2*E*). These results show that the loss of Angptl1 and Angptl2 promotes impaired sprouting of ISVs and increased apoptotic cells around the DA.

Angptl1 and Angptl2 Bind to Endothelial Cells. To clarify the mechanism underlying the *in vivo* phenotype seen in zebrafish after DMO treatment, we performed *in vitro* studies by using HUVECs. First, we generated FLAG-tagged mouse COMP-Angptl1 and -Angptl2 proteins. Although we successfully synthesized the native form of Angptl2, we failed to purify that of Angptl1 because of its unique tendency to aggregate and become insoluble. Although similar difficulties purifying Ang1 have been reported, by replacing the N-terminal portion of Ang1 with a minimal coiled-coil domain from cartilage oligomeric matrix protein (COMP), Koh *et al.* (34, 35) have succeeded in generating a soluble, stable, and potent Ang1 variant, COMP-Ang1 protein. Using the same strategy, we succeeded in generating a soluble and stable Angptl1 variant, COMP-Angptl1. First, we observed monomeric forms of COMP-Angptl1 and -Angptl2 in the presence of reducing agents, 2-mercaptoethanol (2ME), and multimeric forms in nonreducing conditions without 2-mercaptoethanol by Western blotting with an anti-FLAG antibody (Fig. 3*A*). Moreover, we found that COMP-Angptl1 and Angptl2 bound neither Tie1 nor Tie2 (data not shown).

Next, we found that COMP-Angptl1 and Angptl2 show specific binding to HUVECs by FACS analysis. Dose–response binding curves, saturation of binding at a concentration (Fig. 3 *B* and *C*), and greatly decreased binding to other cell types like BaF/3 and Fao (Fig. 10, which is published as supporting information on the PNAS web site) suggested that binding between HUVECs and both proteins was specific, and that the affinity of Angptl2 for HUVECs was greater than that of COMP-Angptl1.

The amino acid sequences of Angptl1 and Angptl2 are very similar between mammalian and zebrafish proteins. Homology is particularly high in the fibrinogen-like domain (Fig. 11, which is published as supporting information on the PNAS web site). Such homology, combined with the fact that the *in vivo* phenotype in zebrafish was particularly robust in double knockdown embryos, suggested a cooperative role of Angptl1 and Angptl2, most likely through a putative common receptor. When HUVECs were pretreated with Angptl2-FLAG, binding of biotinylated COMP-Angptl1 on HUVECs was completely inhibited. In parallel, similar, but partial, inhibition of binding between COMP-Angptl1-FLAG and HUVECs was observed when the converse experiments were performed, (Fig. 12, which is published as supporting information on the PNAS web site). These findings may support a possibility of the cooperative function of Angptl1 and Angptl2 through a common receptor, although further analysis for identifying their cognate receptor will be necessary.

Angptl1 and Angptl2 Possess Antiapoptotic Activity Through the PI3-K/Akt Pathway. When HUVECs were treated with COMP-Angptl1 or Angptl2, phosphorylation of ERK1/2 and Akt was observed, peaking 10 min after treatment (Fig. 3*D*). No effect on BaF/3 and Fao cells was detected (Fig. 13, which is published as supporting information on the PNAS web site). Furthermore, no effect on p38 MAPK and JNK in HUVECs was seen (data not shown). We next examined the biological activities of COMP-Angptl1 and -Angptl2 on HUVECs. Because the ERK1/2

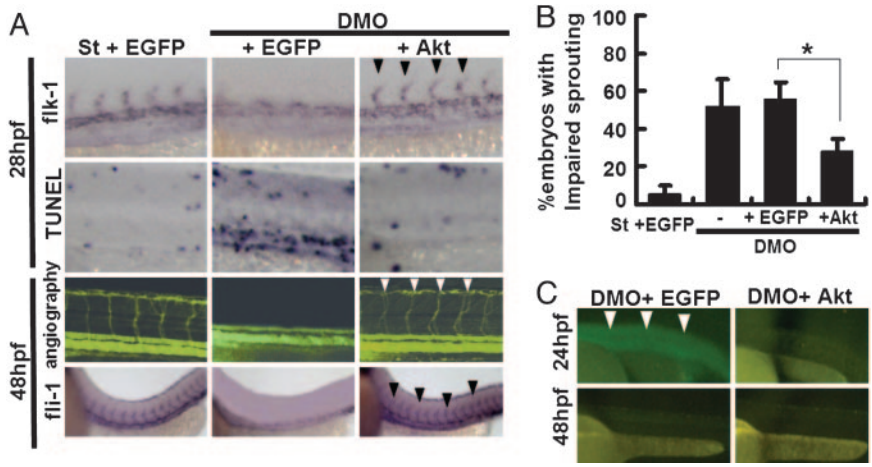

Fig. 4. Coinjection of myristoylated Akt rescues vascular defects in DMO embryos. (*A*) Representative photographs of whole-mount ISH of flk-1 at 28 hpf, whole-mount TUNEL assay at 28 hpf, angiography at 48 hpf, and ISH of fli-1 at 48 hpf. Fifty picograms of EGFP mRNA or myr-Akt mRNA was coinjected into DMO (2 ng each of Angptl1mo and Angptl2mo). As a control, we coinjected 50 pg of EGFP mRNA with 4 ng of the standard morpholino (St plus EGFP). Rescued blood vessels are indicated by filled arrowheads and open arrowheads. (*B*) Percentages of embryos with impaired sprouting of ISVs in five independent experiments ($n = 31–42$ in each experiment) *, $P < 0.01$. (*C*) EGFP activity in the EGFP coinjected group (*Left*) and the myr-Akt coinjected group (*Right*) at 24 hpf and 48 hpf. Open arrowheads indicate abundant EGFP expression in the trunk of an embryo at 24 hpf.

pathway is a major intracellular signaling pathway activated by factors that promote endothelial proliferation, we examined proliferative activity by BrdUrd incorporation. Although VEGF used as a control significantly promoted BrdUrd incorporation, neither COMP-Angptl1 nor Angptl2 stimulated significant increases in BrdUrd incorporation (Fig. 14, which is published as supporting information on the PNAS web site). We next examined antiapoptotic activity of COMP-Angptl1 and -Angptl2 on HUVECs. The numbers of apoptotic cells were significantly decreased in both COMP-Angptl1 and -Angptl2-treated groups based on TUNEL assays (Fig. 3*E*) and Annexin V assays (Fig. 15, which is published as supporting information on the PNAS web site). Finally, to evaluate whether MEK or PI3-K is involved in the antiapoptotic activity of COMP-Angptl1 and -Angptl2, we reexamined apoptotic activity in the presence of their respective inhibitors, PD98059 or LY294002. As compared with controls treated with equivalent amounts of DMSO, LY294002, but not PD98059, significantly inhibited antiapoptotic activity of Comp-Angptl1 and Angptl2 as seen in TUNEL and AnnexinV assays (Figs. 3*E* and 15). These findings suggest that antiapoptotic activity on HUVECs induced by COMP-Angptl1 and -Angptl2 is mediated by the PI3-K/Akt pathway.

Coinjection of Constitutive Active Akt Rescues Vascular Defects Induced by Loss of Angptl1 and Angptl2. Based on our *in vitro* studies, we examined whether activation of Akt by coinjection of myristoylated Akt-1/PKBα mRNA (myr-Akt) rescued the vascular defects seen in DMO embryos. First, by titration experiments, we found a 50-pg injection was the appropriate dose for rescue experiments. Higher doses of Akt mRNA produced severe defects leading to early lethality (data not shown). At the optimal dose, up-regulated Akt/PKB activity rescued impaired angiogenesis seen in the DMO group. As a control, coinjection of the equivalent amount of EGFP mRNA did not rescue defects (Fig. 4 *A* and *B*). Although coinjected EGFP activity was almost undetectable at 48 hpf, we detected abundant EGFP expression in the trunks of embryos at 24 hpf (Fig. 4*C*), suggesting that myr-Akt mRNA is likely active at 24 hpf when sprouting of ISVs occurs.

Discussion

In previous reports, Angptl1 and Angptl2 were shown to possess pro- or antiangiogenic activity. However, there are few reports regarding the physiological role of either protein *in vivo*. In this report, a morpholino antisense strategy in zebrafish showed that Angptl1 and Angptl2 function cooperatively in embryonic angiogenesis through antiapoptotic activity. In addition, both Angptl1 and Angptl2 activate PI3-K/Akt and inhibit apoptosis in cultured endothelial cells. Furthermore, we showed that activation of Akt could rescue the vascular defects induced by loss of Angptl1 and Angptl2.

Recently, we showed that in zebrafish *Zangptl1* is expressed in the myotome, and *Zangptl2* is expressed mainly in the spinal cord and yolk syncytial layer at the time angiogenesis occurs (25). In this report, we demonstrate that loss of function of both proteins leads to vascular defects, specifically in the sprouting of ISVs. ISVs sprout and extend toward the dorsal side of embryos between the myotome and spinal cord. Therefore, one hypothesis is that Angptl1 and Angptl2 secreted from nearby structures acts together on endothelial cells of ISVs as survival factors through activation of the PI3-K/Akt pathway.

In initial reports, Kim *et al.* (11, 12) reported that both Angptl1 and Angptl2 have significant but weak endothelial cell-sprouting activities *in vitro*. Later, it was reported that Angptl1 inhibited VEGF-induced angiogenesis, and it was thus named "Angioarrestin" (16). These authors also proposed that not only Angptl1 but Angptl2 might be antiangiogenic factors. In our hands, Angptl1 stimulated phosphorylation of ERK1/2 and Akt and had significant antiapoptotic activity on HUVECs. Angptl1 may function as either a pro- or antiangiogenic factor, depending on cell context, and it is possible that the primary function of Angptl1 on endothelial cells is an antiapoptotic activity, not an effect on proliferation and sprouting. Our *in vivo* results obtained in zebrafish support that hypothesis: minor vascular defects were seen in Angptl2 knockdown embryos, whereas Angptl1 knockdown embryos showed few vascular abnormalities. Based on the severe defects seen in double knockdown embryos, we suggest that Angptl1 may play a regulatory role for the dominant function of Angptl2 in the process of angiogenesis; Angptl1 may exhibit proangiogenic activity particularly in the absence of Angptl2.

Angiopoietins have been shown to play critical antiapoptotic roles in mammals, similar to findings reported here concerning zebrafish Angptl1 and Angptl2. Our findings prompted us to initiate comparative studies between Angiopoietins and Angptl

families. The genes encoding zebrafish Ang1 (*Zang1*) and Ang2 (*Zang2*) are expressed in the mesenchyme surrounding major trunk vessels (36). Notably, zebrafish Tie-2 is abundantly expressed in postcardinal vein, but not in the DA (37), whereas differences of expression patterns of Tie2 between the DA and postcardinal vein are not seen in mammals. Our data in zebrafish shows that the effect of loss of Angptl1 and Angptl2 was predominantly in arterial angiogenesis. It is important to determine whether Angiopoietin and Angptl signaling are transduced differentially in arterial and venous angiogenesis in zebrafish.

In conclusion, we have shown that the cooperative interactions of Angptl1 and Angptl2 are required for vascular development of zebrafish *in vivo*. We have also shown that Angptl1 and Angptl2 bind to the endothelial cells and both have antiapoptotic activities through the PI3-K/Akt pathway *in vitro*. Identification of a receptor of Angptl1 and Angptl2 is essential for the further analysis of the functional relationships between Angiopoietins and Angptls.

This work was supported by grants-in-aid from the Human Frontiers Science Promotion and the Ministry of Education, Culture, Sports, Science, and Technology of Japan, by a research grant from the Mochida Memorial Foundation for Medical and Pharmaceutical Research, and by a Keio University grant-in-aid for Encouragement of Young Medical Students.

1. Suri, C., Jones, P. F., Patan, S., Bartunkova, S., Maisonpierre, P., Davis, S., Sato, T. N. & Yancopoulos, G. D. (1996) *Cell* **87,** 1171–1180.
2. Sato, T. N., Tozawa, Y., Deutsch, U., Wolburg-Buchholz, K., Fujiwara, Y., Gendron-Maguire, M., Grigley, T., Wolburg, H., Risau, W. & Qin, Y. (1995) *Nature* **376,** 70–74.
3. Lobov, I. B., Brooks, P. C. & Lang, R. A. (2002) *Proc. Natl. Acad. Sci. USA.* **99,** 11205–11210.
4. Koblizek, T. I., Weiss, C., Yancopoulos, G. D., Deutsch, U. & Risau, W. (1998) *Curr. Biol.* **8,** 529–532.
5. Witzenbichler, B., Maisonpierre, P. C., Jones, P., Yancopoulos, G. D. & Isner, J. M. (1998) *J. Biol. Chem.* **273,** 18514–18521.
6. Papapetropoulos, A., Garcia-Cardena, G., Dengler, T. J., Maisonpierre, P. C., Yancopoulos, G. D. & Sessa, W. C. (1999) *Lab. Invest.* **79,** 213–223.
7. Kwak, H. J., So, J.-N., Lee, S. J., Kim, I. & Koh, G. Y. (1999) *FEBS Lett.* **448,** 249–253.
8. Ito, Y., Oike, Y., Yasunaga, K., Hamada, K., Miyata, K., Matsumoto, S., Sugano, S., Tanihara, H., Masuho, Y. & Suda, T. (2003) *Cancer Res.* **63,** 6651–6657.
9. Oike, Y., Yasunaga, K., Ito, Y., Matsumoto, S., Maekawa, H., Morisada, T., Arai, F., Nakagata, N., Takeya, M., Masuho, Y. & Suda, T. (2003) *Proc. Natl. Acad. Sci. USA* **100,** 9494–9499.
10. Oike, Y., Ito, Y., Maekawa, H., Morisada, T., Kubota, Y., Akao, M., Urano, T., Yasunaga, K. & Suda, T. (2004) *Blood* **103,** 3760–3765.
11. Kim, I., Kwak, H. J., Ahn, J. E., So, J. N., Liu, M., Koh, K. N. & Koh, G. Y. (1999) *FEBS Lett.* **443,** 353–356.
12. Kim, I., Moon, S. O., Koh, K. N., Kim, H., Uhm, C. S., Kwak, H. J., Kim, N. G. & Koh, G. Y. (1999) *J. Biol. Chem.* **274,** 26523–26528.
13. Kim, I., Kim, H. G., Kim, H., Kim, H. H., Park, S. K., Uhm, C. S., Lee, Z. H. & Koh, G. Y. (2000) *Biochem. J.* **346,** 603–610.
14. Camenisch, G., Pisabarro, M. T., Sherman, D., Kowalski, J., Nagel, M., Hass, P., Xie, M. H., Gurney, A., Bodary, S., Liang, X. H., *et al.* (2002) *J. Biol. Chem.* **277,** 17281–17290.
15. Le Jan, S., Amy, C., Cazes, A., Monnot, C., Lamande, N., Favier, J., Philippe, J., Sibony, M., Gasc, J. M., Corvol, P., *et al.* (2003) *Am. J. Pathol.* **162,** 1521–1528.
16. Dhanabal, M., LaRochelle, W. J., Jeffers, M., Herrmann, J., Rastelli, L., McDonald, W. F., Chillakuru, R. A., Yang, M., Boldog, F. L., Padigaru, M., *et al.* (2002) *Cancer Res.* **62,** 3834–3841.
17. Chan, J., Bayliss, P. E., Wood, J. M. & Roberts, T. M. (2002) *Cancer Cell* **1,** 257–267.
18. Lee, P., Goishi, K., Davidson, A. J., Mannix, R., Zon, L. & Klagsbrun, M. (2002) *Proc. Natl. Acad. Sci. USA* **99,** 10470–10475.
19. Liao, W., Bisgrove, B. W., Sawyer, H., Hug, B., Bell, B., Peters, K., Grunwald, D. J. & Stainier, D. Y. (1997) *Development (Cambridge, U.K.)* **124,** 381–389.
20. Liao, E. C., Paw, B. H., Oates, A. C., Pratt, S. J., Postlethwait, J. H.& Zon, L. I. (1998) *Genes Dev.* **12,** 621–626.
21. Zhong, T. P., Childs, S., Leu, J. P. & Fishman, M. C. (2001) *Nature* **414,** 216–220.
22. Zhong, T. P., Rosenberg, M., Mohideen, M. A., Weinstein, B. M. & Fishman, M. C. (2000) *Science* **287,** 1820–1824.
23. Lawson, N. D., Vogel, A. M. & Weinstein, B. M. (2002) *Dev. Cell* **3,** 127–136.
24. Lawson, N. D., Scheer, N., Pham, V. N., Kim, C. H. & Chitnis, A. B. (2001) *Development (Cambridge, U.K.)* **128,** 3675–3683.
25. Kubota, Y., Oike, Y., Satoh, S., Tabata, Y., Niikura, Y., Morisada, T., Akao, M., Urano, T., Ito, Y., Miyamoto, T., *et al.* (2005) *Gene Expr. Patterns* **5,** 679–685.
26. Nasevicius, A. & Ekker, S. C. (2000) *Nat. Genet.* **26,** 216–220.
27. Chen, E., Hermanson, S. & Ekker, S. C. (2004) *Blood* **103,** 1710–1719.
28. Westerfield, M. (1994) *The Zebrafish Book: A Guide for the Laboratory Use of Zebrafish* (University of Oregon Press, Eugene, OR).
29. Nasevicius, A., Larson, J. & Ekker, S. C. (2000) *Yeast* **17,** 294–301.
30. Jowett, T. (1999) *Methods Cell. Biol.* **59,** 63–85.
31. Abdelilah, S., Mountcastle-Shah, E., Harvey, M., Solnica-Krezel, L., Schier, A. F., Stemple, D. L., Malicki, J., Neuhauss, S. C., Zwartkruis, F., Stainier, D. Y., *et al.* (1996) *Development (Cambridge, U.K.)* **123,** 217–227.
32. Maekawa, H., Oike, Y., Kanda, S., Ito, Y., Yamada, Y., Kurihara, H., Nagai, R. & Suda T. (2003) *Arterioscler. Thromb. Vasc. Biol.* **23,** 2008–2014.
33. Ramaswamy, S., Nakamura, N., Vazquez, F., Batt, D. B., Perera, S., Roberts, T. M. & Sellers, W. R. (1999) *Proc. Natl. Acad. Sci. USA* **96,** 2110–2115.
34. Cho, C.-H., Kammerer, R. A., Lee, H. J., Steinmetz, M. O., Ryu, Y. S., Lee, S. H., Yasunaga, K., Kim, K.-T., Kim, I., Choi, H.-H., *et al.* (2004) *Proc. Natl. Acad. Sci. USA* **101,** 5547–5552.
35. Cho, C.-H., Kammerer, R. A., Lee, H. J., Yasunaga, K., Kim, K.-T., Choi, H.-H., Kim, W., Kim, S. H., Park, S. K., Lee, G. M. & Koh, G. Y. (2004) *Proc. Natl. Acad. Sci. USA* **101,** 5553–5558.
36. Pham, V. N., Roman, B. L. & Weinstein, B. M. (2001) *Dev. Dyn.* **221,** 470–474.
37. Lyons, M. S., Bell, B., Stainier, D. & Peters, K. G. (1998) *Dev. Dyn.* **212,** 133–140.